

Error Prediction for Adaptive Modulation and Coding in Multiple-Antenna OFDM systems

Sébastien Simoens, Stéphanie Rouquette-Léveil ^{*} ;
Philippe Sartori, Yufei Blankenship, Brian Classon [†]
e-mail: simoens@motorola.com

January 10, 2005

Abstract

In this paper, the problem of Packet Error Rate prediction is addressed in the multiple-antenna broadband OFDM context, and its impact on Adaptive Modulation and Coding (AMC) is quantified. The analysis is based on a physical layer comprising various modulation and coding schemes, ranging from robust space-time block coding (STBC) modes to high bit rate spatial division multiplexing (SDM) modes, and also hybrid SDM-STBC schemes. For each mode the expression of several Link Quality Metrics enabling PER prediction in the broadband OFDM channel, such as instantaneous SNR, capacity, or exponential effective SNR metrics are provided. Their advantages and limitations are investigated. Finally, their performance is benchmarked in the IEEE 802.11a/g/n context. It is shown that the choice of the Link Quality Metric has a significant impact on the throughput performance of the AMC algorithm.

^{*}Motorola Labs, Parc Les Algorithmes, St-Aubin 91193 Gif-sur-Yvette, FRANCE.

[†]Motorola Labs, MOTOROLA INC, 1301 E Algonquin Road, Schaumburg IL 60196-1078 USA

Contents

1	Introduction	3
2	Multiple-Antenna OFDM Physical Layer description	5
2.1	Description of the transmitter	5
2.2	Receiver processing	6
2.2.1	Alamouti STBC	7
2.2.2	Spatial Division Multiplexing modes	8
2.2.3	Hybrid SDM-STBC modes	8
3	AMC algorithm and PER prediction	9
3.1	Instantaneous SNR	9
3.2	Shannon Capacity expression	9
3.3	Exp-ESM methodology	10
4	Performance comparison	11
4.1	Accuracy of the LQMs	11
4.2	Impact on system throughput	12
5	Conclusion	14

1 Introduction

The bit rate offered by wireless communication systems has dramatically increased recently. Short range Wireless Local Area Networks (WLANs) such as IEEE 802.11a/g [11] or large range Metropolitan Area Networks (WMANs) such as IEEE 802.16 both offer tens of megabits per second raw bit rate. The dominant transmission technique in these standardization areas is Orthogonal Frequency Division Multiplexing (OFDM) [12] associated with Bit Interleaved Coded Modulation (BICM) [13]. In BICM-OFDM, information bits are coded (e.g., convolutionally) and punctured, interleaved, then mapped onto complex symbols (e.g., QAM). The OFDM modulator/demodulator processes blocks of symbols using IFFT/FFT. Thanks to a prepended guard interval (GI) (more precisely a cyclic prefix), the multipath propagation channel is turned into an equivalent set of parallel flat-fading channels. The association of a coding rate and a constellation size determines a Modulation and Coding Scheme (MCS) which has a given bit rate. The task of Adaptive Modulation and Coding (AMC) is to select the best MCS for the current radio link quality so as to achieve higher system throughput. For instance in IEEE 802.11a/g, eight MCS are defined ranging from BPSK with code rate $R=1/2$, offering a bit rate of 6 Mb/s at the physical (PHY) layer, to 64QAM rate $R=3/4$ offering 54Mb/s.

There are several approaches that may be considered in order to further increase the PHY bit rate. A simple approach is to increase the bandwidth. However, spectrum remains a limited resource and it is difficult to make broad bands available for a service around the world. Furthermore, increasing bandwidth requires the transmitted signal power to be increased in the same proportion, in order to maintain cell range. Another approach is to increase the coding rate or constellation order, but it is difficult because it requires the radio device to achieve a higher signal to noise plus distortion ratio. The approach investigated in this paper is the use of multiple-antenna transmissions because a very high spectrum efficiency can be achieved especially in rich scattering propagation environments, as shown in [14] and [15]. Moreover, multiple-antenna processing can be easily associated with OFDM, thanks to the equivalent parallel channel model. The capacity of MIMO-OFDM is studied in details in [15]. Moreover, various transmission schemes can be considered for a given multiple antenna configuration. Some schemes such as spatial division multiplexing (SDM) can rely on the transmission of several bit streams (e.g. one bit stream per transmit antenna) per OFDM subcarrier. Other schemes such as Space Time Block Coding (STBC) [16], transmit the same bit at different times on different antennas in order to increase the diversity and thus the robustness. The SDM modes tend to provide high bit rate at short distance, while STBC modes provide lower bit rate with higher range. Open-loop schemes assume no prior knowledge of the channel state at the transmitter, while closed-loop schemes assume a certain knowledge of the channel state obtained either explicitly by receiver feedback, or implicitly assuming channel reciprocity. A transmitter operating in closed-loop mode can even perform the Singular Value Decomposition

of the channel matrix for each subcarrier and optimize the power and constellation size per channel eigenmode. This approach involves both the water-pouring and bit-loading concepts [17]. Obviously, the design of an efficient AMC algorithm is made even more difficult in multiple-antenna systems. This paper is restricted to the study of open-loop techniques either based on SDM, STBC or on hybrid SDM-STBC schemes. In addition to the constellation and coding rate, the AMC has to select among the multiple-antenna techniques (SDM, STBC, . . .) available for the $N_t \times N_r$ antenna setting, where N_t (resp. N_r) is the number of transmit (resp. receive) antennas.

As explained in this paper, the AMC algorithm tries to maximize the throughput available on top of the Medium Access Control (MAC) layer, under some QoS constraints like packet delivery delay. The PHY layer Packet Error Rate (PER) determines the statistics of the number of retransmissions which ultimately determine both throughput and delay. Therefore, the AMC will try to meet a target PER while selecting the highest possible bit rate. Note that in this paper AMC is applied on a single link, so that AMC only relies on PER prediction. However, per-link PER predictions would also be a very important input should a joint AMC - resource allocation algorithm be considered. The AMC must base its decision on the best PER prediction for the various MCS at the time the next packet will be transmitted. A simple approach is to estimate the PER by dividing the number of erroneous packets by the total number of received packets during a given observation window. However, such an estimator assumes a slow-varying channel and takes too many packets to converge, especially at low PER values. Faster convergence and more accurate estimate can be expected by predicting the future Channel State Information (CSI) and deriving a PER estimate from the predicted CSI. The predictor can rely on the knowledge of channel statistics (e.g. Kalman filtering). As illustrated in this paper, the derivation of the PER estimate from the channel prediction has a strong impact on system performance. In a noise limited environment, it can be assumed that the PER is a function of the MCS, the noise variance and the complex channel coefficients matrix. The number of dimensions of this function is huge, and many attempts have been made in the literature to map these parameters onto a single Link Quality Metric (LQM) which could be associated to the PER by means of a look-up table obtained either by simulation or real hardware measurements.

For instance, the instantaneous Signal to Noise Ratio (SNR) was used in [4]. In a single antenna OFDM system, it depends on the average of the squared modulus of the complex channel coefficients on every subcarrier. However, it was shown in [5] that the PER vs instantaneous SNR performance of a given MCS could still differ significantly from one multipath channel realization to another. Therefore, if the AMC is based on instantaneous SNR, there are some 'bad' channels for which the AMC may select a bit rate which exhibits a PER much higher than the target PER in the current propagation conditions. Since the channel coherence time

in a WLAN can be very long (hundreds of ms), the link could be practically broken. A solution to this problem can be to conservatively shift the SNR thresholds used by the AMC by a few dBs. In order to reduce this margin, the authors in [5] define an 'effective SNR' which depends not only on the average, but also on the variance of the channel coefficients magnitude. In [6], the effective SNR is derived from the union bound applied to a convolutionally-coded system. Among the LQMs taking into account forward error correction (FEC) effects, the exponential effective SNR mapping [7] represents a good performance/complexity trade-off. Shannon Capacity can also be used as a LQM, as proposed in [8], but has the drawback that it cannot account for FEC.

In this paper, the impact of PHY PER prediction on MAC throughput performance is shown. Three LQMs are benchmarked, namely instantaneous SNR, Shannon Capacity and exp-ESM effective SNR versus an ideal AMC with perfect PER prediction. It is shown how multiple-antenna processing affects the computation of each LQM. In section 2, the Physical layer on which the AMC algorithm will operate is described. In section 3, the AMC algorithm and the expression of the associated LQMs are detailed. In section 4, the throughput performance of the AMC based on the various LQMs is illustrated, before drawing conclusions in section 5.

2 Multiple-Antenna OFDM Physical Layer description

In order to illustrate the system impact of PER prediction for AMC, the complete Physical layer offering various bit rates, multiple-antenna configurations and coding schemes, on which the system relies, is described.

2.1 Description of the transmitter

The PHY layer described hereafter was proposed in the framework of IEEE 802.11n standardization and is described in details in [18]. The transmit chain is described on Figure 1. The data bits are scrambled, convolutionally encoded with mother code rate $R=1/2$, punctured to rates varying between $R=1/2$ and $R=5/6$, and frequency interleaved. Then groups of successive bits are mapped onto QAM symbols (BPSK to 64QAM). The space/time encoding and interleaving are applied per OFDM subcarrier. Finally, OFDM modulation and cyclic prefix insertion are performed prior to digital to analog conversion, up-conversion, and emission of the RF signal on each antenna.

As mentioned before, the proposed PHY layer includes various space-time encoding schemes, which are applied per OFDM subcarrier. Several possible antenna configurations are depicted on Figures 2, 3 and 4. They differ in the number of parallel streams simultaneously transmitted, thus allowing robust modes with low to medium data rates, as well as high data rate modes under good channel conditions. This objective is achieved by using various multiple-antenna

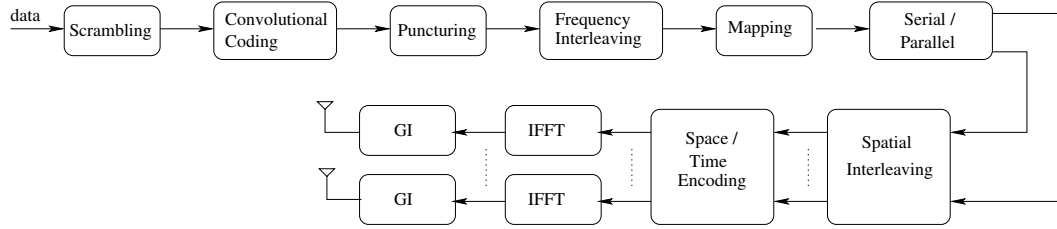


Figure 1: Multiple-antenna OFDM transmitter.

techniques, including STBC, SDM, and hybrid transmission schemes presenting a trade-off between pure Alamouti coding [1] and pure SDM approaches. As an example, when using four transmit antennas, the first hybrid approach consists in transmitting two parallel Alamouti codes on four antennas [2] [3], and the second hybrid approach in transmitting one Alamouti coded stream in parallel with uncoded streams on the third and fourth antennas (see Figure 4). For pure SDM schemes, it is assumed that the number of transmitted independent bit streams equals the number of transmit antennas.

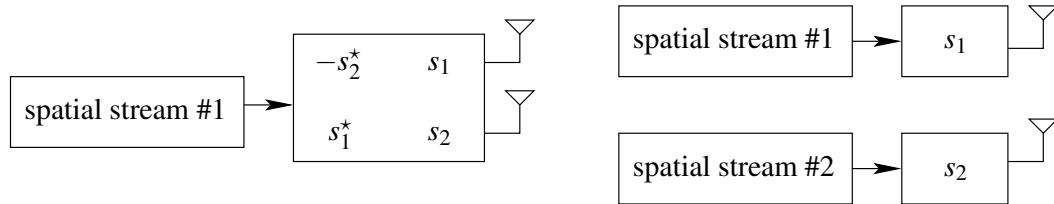


Figure 2: Space-Time coding schemes proposed for 2 transmit antennas (left: Alamouti STBC, right: SDM).

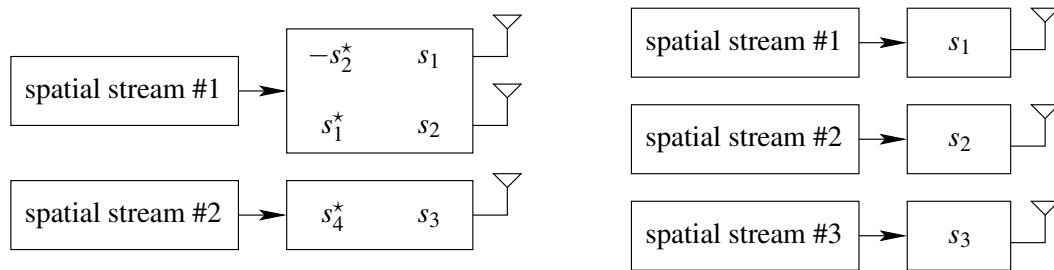


Figure 3: Space-Time coding schemes proposed for 3 transmit antennas (left: Hybrid SDM-STBC, right: SDM).

2.2 Receiver processing

In all the space-time coding schemes described on Figures 2, 3 and 4, a certain number of QAM symbols s_i are sent over one or two successive OFDM symbols. In order to recover the

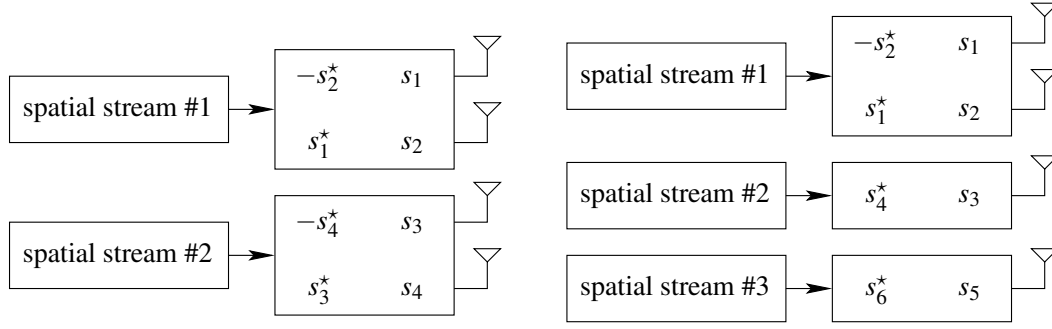


Figure 4: Space-Time coding schemes proposed for 4 transmit antennas.

initial bit stream, many processing schemes can be applied at the receiver. In low complexity receivers, a linear space-time processing step is performed on each subcarrier, and the noisy output symbols are demapped into bit metrics which are depunctured, deinterleaved and fed to the Viterbi decoder. The focus in this paper is on ZF and MMSE linear receivers, but the same methodology applies for any receiver processing scheme. Denote by N_t (resp. N_r) the number of transmit (resp. receive) antennas. Denote by \mathbf{H} the $N_r \times N_t$ channel matrix on a given subcarrier. For notational simplicity, the dependence on subcarrier index is neglected in this section. The channel is assumed to remain constant over the whole packet. Therefore, $H_{m,n}$ is the channel coefficient from Tx antenna n to Rx antenna m . The noise variance per receive antenna is denoted by σ^2 . The transmit power is uniformly distributed over the transmit antennas such that the signal variance per antenna is $\frac{P_t}{N_t}$. N_s is the number of independent bit streams. Also, y_m^i and n_m^i denote the complex received symbol and noise on antenna m for OFDM symbol i .

2.2.1 Alamouti STBC

For Alamouti STBC modes with $N_t = 2$ transmit antennas, it is well known that after conjugating the first received symbol y_m^1 , an orthogonal equivalent channel matrix can be formed as follows:

$$\begin{bmatrix} y_m^{1*} \\ y_m^2 \end{bmatrix} = \begin{bmatrix} H_{m,2}^* & -H_{m,1}^* \\ H_{m,1} & H_{m,2} \end{bmatrix} \begin{bmatrix} s_1 \\ s_2 \end{bmatrix} + \begin{bmatrix} n_m^{1*} \\ n_m^2 \end{bmatrix} \quad (1)$$

Therefore, the receiver multiplies $[y_m^{1*} \ y_m^2]^t$ by the hermitian transpose of the equivalent channel matrix to recover s_1 and s_2 scaled by $|H_{m,1}|^2 + |H_{m,2}|^2$. Maximum Ratio Combining (MRC) can then be applied by simply summing over the N_r receive antennas. Finally, the signal to noise ratio at the output of the MRC is:

$$\gamma = \frac{P_t}{\sigma^2 N_t} \sum_{n=1}^2 \sum_{m=1}^{N_r} |H_{m,n}|^2 \quad (2)$$

2.2.2 Spatial Division Multiplexing modes

For SDM modes, many linear (e.g. ZF, MMSE) and non-linear (e.g. V-BLAST) processings are possible. In this paper, the focus is on linear processing only. The received $N_r \times 1$ symbol vector $\mathbf{y}^1 = [y_1^1, \dots, y_{N_r}^1]^t$ is multiplied by a matrix \mathbf{W} . For ZF processing, \mathbf{W} is the pseudo-inverse of \mathbf{H} :

$$\mathbf{W} = (\mathbf{H}^H \mathbf{H})^{-1} \mathbf{H}^H \quad (3)$$

For MMSE processing:

$$\mathbf{W} = \mathbf{H}^H \left(\mathbf{H} \mathbf{H}^H + \sigma^2 \frac{N_t}{P_t} \mathbf{I}_{N_r} \right)^{-1} \quad (4)$$

Denoting by $\mathbf{s} = [s_1, s_2, \dots, s_{N_s}]^t$ the $N_s \times 1$ vector of sent symbols, and \mathbf{n} the thermal noise vector, the output after ZF processing equals:

$$\mathbf{z} = \mathbf{s} + \mathbf{W} \mathbf{n} \quad (5)$$

After ZF processing, the output is affected by a colored noise of covariance matrix:

$$\mathbf{R} = \sigma^2 \mathbf{W} \mathbf{W}^H \quad (6)$$

In the rest of the paper, the focus is on the more complex MMSE case, where the output can be expressed as:

$$\mathbf{z} = \mathbf{W} \mathbf{H} \mathbf{s} + \mathbf{W} \mathbf{n} = \text{diag}(\mathbf{W} \mathbf{H}) \mathbf{s} + (\mathbf{W} \mathbf{H} - \text{diag}(\mathbf{W} \mathbf{H})) \mathbf{s} + \mathbf{W} \mathbf{n} \quad (7)$$

The output is affected by a colored noise, plus inter-stream interference. In the following, this interference is approximated as additive gaussian noise, and the overall noise plus interference covariance matrix equals:

$$\mathbf{R} = \frac{P_t}{N_t} (\mathbf{W} \mathbf{H} - \text{diag}(\mathbf{W} \mathbf{H})) (\mathbf{W} \mathbf{H} - \text{diag}(\mathbf{W} \mathbf{H}))^H + \sigma^2 \mathbf{W} \mathbf{W}^H \quad (8)$$

The N_s Signal to Noise plus Interference ratio vector at the output of MMSE processing is thus:

$$\gamma = \frac{P_t}{N_t} \text{diag}(\mathbf{W} \mathbf{H}) \text{diag}(\mathbf{W} \mathbf{H})^H \text{diag}(\mathbf{R})^{-1} \quad (9)$$

2.2.3 Hybrid SDM-STBC modes

For the linear processing of these modes, two successive $N_r \times 1$ received symbol vectors \mathbf{y}^1 and \mathbf{y}^2 are processed, in order to recover the two $N_s \times 1$ QAM symbol vectors \mathbf{s}^1 and \mathbf{s}^2 . Denote by $\mathbf{h}_n = (H_{1,n}, \dots, H_{N_r,n})^t$ the $N_r \times 1$ channel coefficients from transmit antenna n . The focus in this subsection is on the hybrid scheme of Figure 3, where $N_t = 3$, $N_r = 2$ and $N_s = 2$ but the methodology remains the same for other hybrid schemes. The principle is to construct a code

such that an equivalent channel matrix \mathbf{H}_e can be formed with a rank high enough to solve the linear system in the least squares sense. The received signal vector is:

$$\begin{bmatrix} \mathbf{y}^{1*} \\ \mathbf{y}^2 \end{bmatrix} = \underbrace{\begin{bmatrix} \mathbf{h}_2^* & -\mathbf{h}_1^* & \mathbf{0} & \mathbf{h}_3^* \\ \mathbf{h}_1 & \mathbf{h}_2 & \mathbf{h}_3 & \mathbf{0} \end{bmatrix}}_{\mathbf{H}_e} \begin{bmatrix} \mathbf{s}^1 \\ \mathbf{s}^2 \end{bmatrix} + \begin{bmatrix} \mathbf{n}^{1*} \\ \mathbf{n}^2 \end{bmatrix} \quad (10)$$

Just like in section 2.2.2, a signal to noise ratio can be computed at the output of the ZF and MMSE detectors. Equations remain the same except that \mathbf{H} must be replaced by \mathbf{H}_e .

3 AMC algorithm and PER prediction

As explained in the introduction, the ideal LQM is a function which maps the channel matrix and the noise variance onto a scalar which can be straightforwardly associated to the PER via a look-up table. The look-up table depends on the MCS and on the packet length. The LQM function itself can also depend on the MCS. For instance, the mutual information ideally depends on the signal distribution, hence on the constellation. Likewise, the union bound depends on the convolutional code transfer function. In this section, the three candidate LQMs that will be benchmarked in section 3.3 are presented. The equivalent channel matrices and signal to noise ratios after space-time receiver processing derived in section 2.2 are used. However, the dependence on the OFDM subcarrier index previously removed for notational simplicity is reintroduced. Consequently, \mathbf{H}^j , \mathbf{W}^j , \mathbf{R}^j and γ^j are related to the j th subcarrier among the N_u useful data subcarriers. Note that in 802.11a/g, $N_u = 48$.

3.1 Instantaneous SNR

This is a simple LQM developed for single antenna. In order to keep the LQM a scalar, its definition is extended to multiple-antennas by averaging over the receiver antennas:

$$SNR_{instant} = \frac{P_t}{N_u N_r N_t \sigma^2} \sum_{j=1}^{N_u} \sum_{m=1}^{N_r} \sum_{n=1}^{N_t} |H_{m,n}^j|^2 \quad (11)$$

Note however that the SNR per receive antenna would have more signification for an RF front-end designer.

3.2 Shannon Capacity expression

The general expression for OFDM-MIMO channel capacity proposed in [15] is:

$$C = \sum_{j=1}^{N_u} \log \left(\mathbf{I}_{N_r} + \frac{P_t}{\sigma^2 N_t} \mathbf{H}^j \mathbf{H}^{jH} \right) \quad (12)$$

The capacity indicates the maximum spectrum efficiency that could ideally be reached assuming uncorrelated Gaussian signal on each transmit antenna and ideal channel coding. Clearly, none of these assumptions holds in a real system and it can be verified that the straightforward application of equation (12) as a LQM does not provide good results.

A possible improvement is to consider a channel which encompasses the space-time encoder and decoder. In that case, a different LQM formula is used for each space-time coding scheme. For Alamouti STBC, the signal to noise ratio at the output of the channel is given by equation (2) and the capacity can be expressed as:

$$C = \sum_{j=1}^{N_u} \log \left(1 + \frac{P_t}{2\sigma^2} \sum_{n=1}^2 \sum_{m=1}^{N_r} |H_{m,n}^j|^2 \right) \quad (13)$$

For SDM, the channel undergoes correlated noise of the covariance matrix given by equation (8). Moreover, one can notice that this noise correlation at the output of the receiver space time processing will be removed after deinterleaving. Therefore, the expression for capacity on such a channel becomes:

$$C = \sum_{j=1}^{N_u} \log \left(\mathbf{I}_{N_t} + \frac{P_t}{N_t} \text{diag}(\mathbf{W}^j \mathbf{H}^j) \text{diag}(\mathbf{R}^j)^{-1} \text{diag}(\mathbf{W}^j \mathbf{H}^j)^H \right) \quad (14)$$

The capacity of hybrid SDM-STBC schemes has an expression very similar to equation (14):

$$C = \frac{1}{2} \sum_{j=1}^{N_u} \log \left(\mathbf{I}_{N_s} + \frac{P_t}{N_t} \text{diag}(\mathbf{W}^j \mathbf{H}_e^j) \text{diag}(\mathbf{R}^j)^{-1} \text{diag}(\mathbf{W}^j \mathbf{H}_e^j)^H \right) \quad (15)$$

3.3 Exp-ESM methodology

The exponential effective SNR mapping method (Exp-ESM) has been proposed to predict PER performance in OFDM systems in [7] and [20]. It consists in deriving a LQM which is called effective SNR, and which is the SNR that would be required on AWGN channel to obtain the same PER. The theoretical justification is derived from the union bound and Chernoff bound, for BPSK and QPSK constellations. For a general MIMO-OFDM system with QAM constellations, a scalar β is found by simulations such that the effective SNR LQM equals:

$$\gamma_{eff} = -\beta \log \left(\frac{1}{N_u N_s} \sum_{j=1}^{N_u} \sum_{i=1}^{N_s} \exp \left(-\frac{\gamma_i^j}{\beta} \right) \right) \quad (16)$$

where γ_i^j is the SNR at the output of space-time processing, for stream i on subcarrier j , and is given by equations (2) and (9). A way to obtain β is to fit the model over a large-enough number of independent channel realizations according to a criterion. One criterion to select the optimum β value is:

$$\beta_{opt} = \min_{\beta} \left(\max_{i,j} (|\gamma_{eff,j} - \gamma_{eff,i}|) \right) \quad (17)$$

where $\gamma_{eff,i}$ is the effective SNR found for the i th independent channel trial. The advantage of exp-ESM over capacity is that it accounts for the FEC without requiring the knowledge of the code transfer function.

4 Performance comparison

In this section, the performance of the three LQMs defined in Section 3 are compared in the single-antenna and multiple-antenna context. Simulations are conducted over 802.11n channel models D and E [9, 10], with twenty independent channel realizations generated for each model.

4.1 Accuracy of the LQMs

In Figure 5, the PER vs Instantaneous SNR curves are superimposed for forty independent channels in a single antenna context for the 64QAM, R=3/4 802.11a/g mode. In this example, the best and worst PER curves are separated by 7 dB. It is concluded that instantaneous SNR is not a good LQM for a multicarrier system.

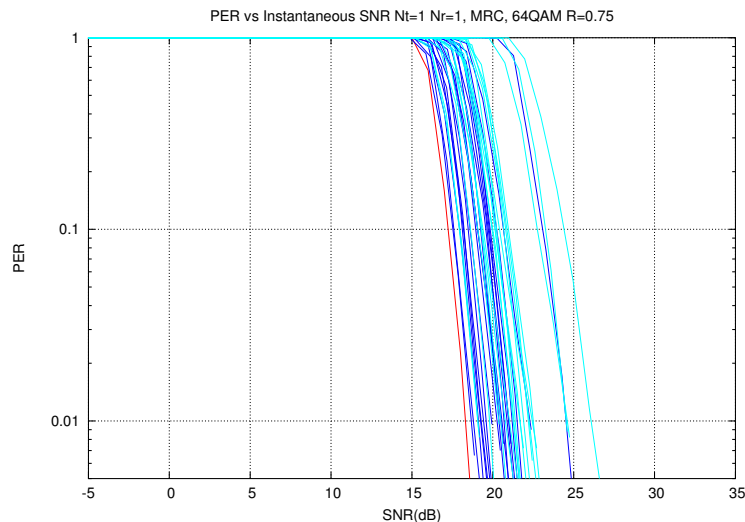


Figure 5: PER vs Instantaneous SNR, single antenna, 64 QAM, R=3/4, 40 independent channel realizations (20 IEEE 802.11n channel D and 20 IEEE 802.11n channel E).

Under the same conditions, exp-ESM and capacity yield a much better matching, as illustrated in Figure 6. It seems that exp-ESM curves match even better, but the accuracy difference cannot be quantified since the abscissa of the two plots in Figure 6 are not the same. One way to compare the LQMs is to measure the effective SNR range after inverting the capacity formula assuming an equivalent AWGN channel, as proposed in [19]. Inverting the capacity matrix is also feasible in multiple-antenna context, since the IEEE 802.11n Task Group has extended the

AWGN reference channel to multiple antenna setting by assuming that the channel matrix is a truncated Fourier transform (i.e. full rank matrix). In this paper the comparison of the three metrics is done in terms of the throughput performance of an AMC algorithm employing each, which is ultimately what matters to the upper layers.

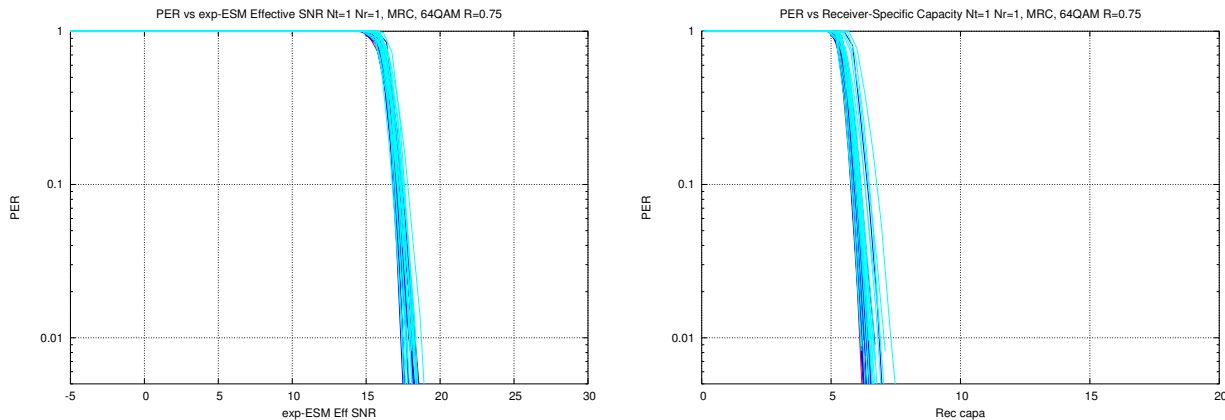


Figure 6: PER vs exp-ESM effective SNR (left) and capacity (right), single antenna, 64 QAM, $R=3/4$, 20 independent IEEE 802.11n channel D and E.

4.2 Impact on system throughput

The role of the PHY layer is to provide a packet delivery service to the MAC layer. The MAC can tolerate a residual PER at the output of the PHY, since these erroneous packets will be identified by CRC and retransmitted by a retransmission (ARQ) protocol. In a WLAN, the delays resulting from the ARQ are low with respect to those tolerated by higher layer protocols (e.g. TCP). Therefore, a large number of retransmissions is possible. Under unlimited retransmissions and neglecting the overhead introduced by the MAC protocol, the throughput ρ for a raw PHY bit rate r equals:

$$\rho = r(1 - PER) \quad (18)$$

An AMC algorithm that selects the MCS with the maximum throughput while meeting the target PER constraint is simulated. According to Figures 5 and 6 there exists a target LQM value corresponding to the target PER for each channel, although ideally the LQM value of different channel realizations should be as close as possible to each other (i.e., the LQM value is independent of the instantaneous channel realization). In order to have a fair and realistic comparison between the various LQMs, the target LQM is defined such that 95% of the channels have a PER lower than the target PER. Also a target PER of 5% is selected, which is a realistic value for MAC performance evaluation.

The throughput vs. average SNR performance of the three LQM is examined in the 802.11a/g context on figure 7. The magenta dotted line represents the throughput obtained with perfect knowledge of the PER for every channel realization and is thus an upper bound on the performance of any PER prediction algorithm. The thin cyan curves represent the average throughput of each mode without AMC, and therefore without any constraint on target PER or outage. The better PER prediction with capacity yields up to 3 dB gain over instantaneous SNR (red vs dashed blue curve), but the prediction remains imperfect, because (among other reasons) the real system including FEC does not operate at capacity. Exp-ESM provides a slight improvement over capacity, but is still sub-optimum. Note that in Figures 5 and 6, the genie does better than the hull of the curves obtained for each MCS. This happens because each of the cyan curve is generated for a fixed MCS (without AMC). The genie curve is generated with perfect PER knowledge and AMC, thus does better than the fixed modulation and coding.

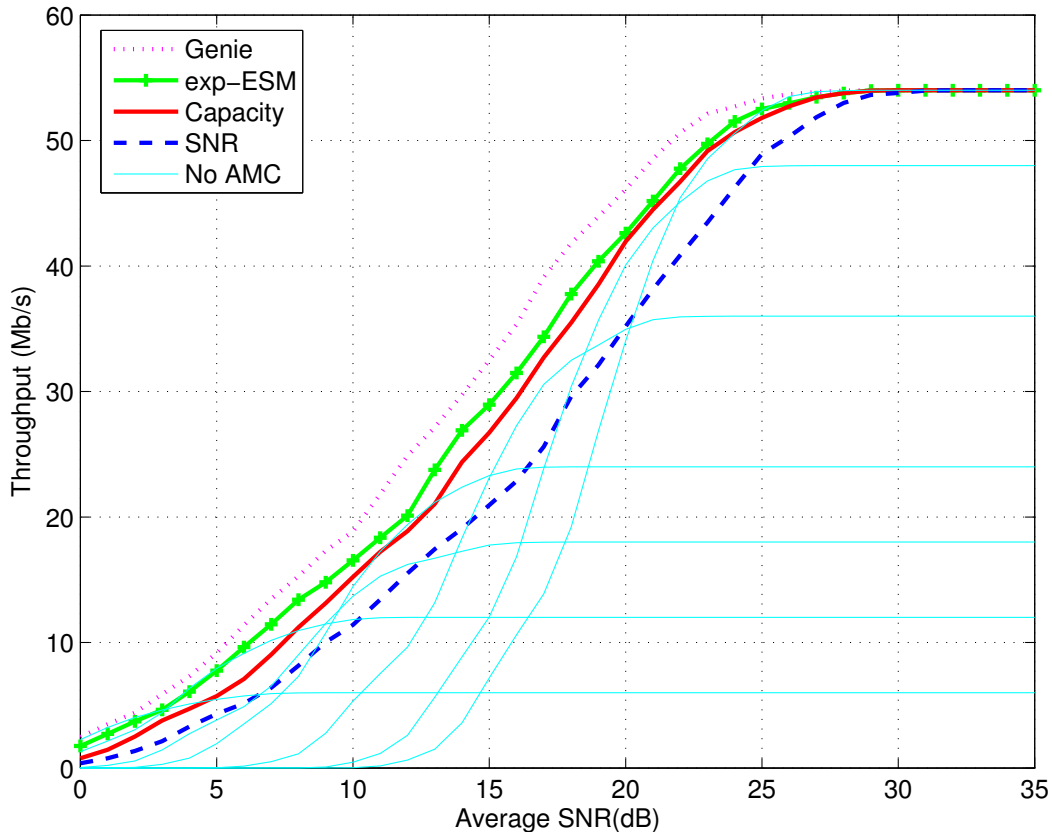


Figure 7: Throughput vs. Average SNR, 802.11a/g system, 802.11n channels D and E models.

In Figure 8, the average throughput is plotted versus average SNR for a $N_t = 2$, $N_r = 2$ system. The seven low bit rate modes rely on Alamouti STBC, whereas the four higher bit rate modes rely on SDM. Only channel model D was used, because the SDM modes can require a

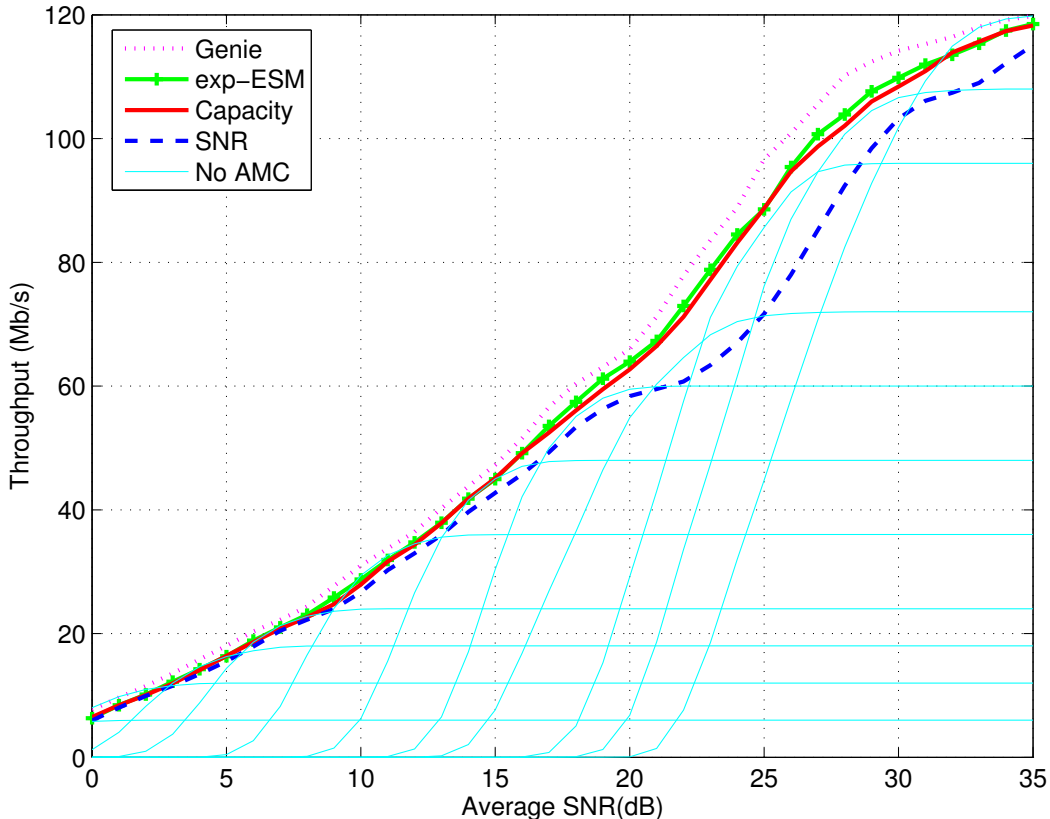


Figure 8: Throughput vs. Average SNR, $N_t = 2, N_r = 2$ system, 802.11n channel D model.

high SNR to meet the target PER constraint that is difficult to reach under realistic conditions with channel E. Indeed, channel E has rays with delays almost as long as the cyclic extension. When convolved with the transmit and receive filters, the global channel impulse response can exceed the cyclic extension, leading to inter-symbol and inter-carrier interference not accounted for in (9). It can be observed in Figure 8 that the three LQMs work very well for Alamouti STBC modes, which is intuitively justified by the fact that this scheme maximizes the diversity, reducing the fading fluctuations with a view to approach the behaviour of an AWGN channel.

5 Conclusion

In this paper, the problem of PER prediction based on various Link Quality Metrics is addressed in the multiple-antenna OFDM context. The analysis is based on a physical layer comprising various modulation and coding schemes, ranging from robust space-time block coding to high bit rate space division multiplexing modes, as well as hybrid SDM-STBC schemes. For all these modes, the expression of the various LQMs is provided and their characteristics are explored. It is shown how they can be applied to the new context of space-time coding techniques. Finally,

the performance of three LQMs is benchmarked and shown to ultimately have a significant impact on the throughput performance of the AMC algorithm. Improvements of the existing LQMs are still possible, as shown by simulations.

References

- [1] S. M. Alamouti, "A Simple Transmit Diversity Technique for Wireless Communications," *IEEE Journal on Selected Areas in Communications*, vol. 16, no. 8, pp. 1451-1458, October 1998.
- [2] Texas Instruments, "Double-STTD scheme for HSDPA systems with four transmit antennas: Link Level Simulation Results," *TSG-R WG1 document, TSGR1#20(01)0458*, May 2001.
- [3] X. Zhuang, F.W. Vook, S. Rouquette-Léveil, and K. Gosse, "Transmit Diversity and Spatial Multiplexing in Four-Transmit-Antenna OFDM," *IEEE Int. Conf. on Comm.*, vol 4, pages 2316–2320, May 2003.
- [4] S. Simoens and D. Bartolomé, "Optimum performance of link adaptation in HIPERLAN/2 networks," *IEEE Vehicular Technology Conference (VTC)*, May 2001.
- [5] Mattias Lampe, Hermann Rohling and Wolfgang Zirwas, "Misunderstandings about Link Adaptation for frequency selective fading channels," *IEEE Personal Indoor Mobile Radio Conference (PIMRC)*, 2002.
- [6] S. Nanda and K. Rege, "Frame Error Rates for Convolutional Codes on Fading Channels and the concept of effective E_b/N_0 ," *IEEE Transactions on Vehicular Technology*, Vol. 47, Nb. 4, Nov 1998.
- [7] Ericsson, "System-Level evaluation of OFDM - Further Considerations," *3GPP TSG-RAN WG1*, Nov 2003.
- [8] FITNESS, "D3.3.1 - MTMR Baseband Transceivers Needs for Intra-system and Inter-system (UMTS/WLAN) Reconfigurability," *IST Information Society Technologies*, Nov 2003.
- [9] 802.11n Task Group, "TGn Channel Models, 802.11-03/940r4," *IEEE P802.11*, May 2004.
- [10] Jean Philippe Kermoal et al. "A Stochastic MIMO Radio Channel Model With Experimental Validation," *IEEE Journal on Selected Areas in Communications*, Vol 20, Nb. 6, Aug 2002.
- [11] IEEE 802.11a "Part 11:Wireless LAN Medium Access Control (MAC) and Physical Layer specifications (PHY) - High Speed Physical Layer in the 5GHz band," *IEEE Standards Department*, Jan 1999.
- [12] B. Le Floch, M. Alard and C. Berrou "Coded orthogonal frequency division multiplex (TV broadcasting)," *Proceedings of the IEEE*, vol. 83, Nb. 6, pages 982–996, June 1995.

- [13] G. Caire and G. Taricco and E. Biglieri “Bit-Interleaved Coded Modulation,” *IEEE Transactions on Information Theory*, Vol. 44, Pages 927–946, May 1998.
- [14] I. Emre Telatar, “Capacity of multi-antenna Gaussian channels,” *European Trans. Telecomm.*, vol. 10, no. 6, pp. 585-595, 1999.
- [15] H. Bölcskei, D. Gesbert and A.J. Paulraj, “On the Capacity of Wireless Systems Employing OFDM-Based Spatial Multiplexing”, *IEEE ICASSP*, June 2000.
- [16] V. Tarokh, H. Jafarkhani and A.R. Calderbank, “Space-Time Block Codes from Orthogonal Designs”, *IEEE Transactions on Information Theory*, Vol. 45, Nb 5, pages 1456–1467, Jul 1999.
- [17] F. Boixadera Espax and J.J. Boutros, “Capacity Considerations for Wireless Multiple-Input Multiple-Output Channels,” *Workshop on Multiaccess, Mobility and Teletraffic for Wireless Communications*, 1999
- [18] Stephanie Rouquette-Leveil et al. “MIMO-based PHY layer techniques for IEEE802.11n,” *12th WWRP meeting*, New-York, USA, Nov 2004.
- [19] J. Kim et al., “On efficient link error prediction based on convex metrics,” *IEEE VTC Fall* , Los Angeles, 2004.
- [20] Y. Blankenship, P. Sartori, B. Classon and K. Baum, “Link Error Prediction Methods for Multicarrier Systems,” *IEEE VTC Fall* , Los Angeles, 2004.